香港天文台
HONG KONG OBSERVATORY

Reprint 1354

Applications of Nuclear Accident Consequence Assessment System during the episode of Mangkhut (1822)

LEUNG Wai-hung, MA Wai-man, and NG Chun-yuen

The 33rd Guangdong - Hong Kong - Macao Seminar
on Meteorological Science and Technology
and
The 24th Guangdong - Hong Kong - Macao Meeting
on Cooperation in Meteorological Operations

(Hong Kong 6-8 March 2019)

山竹(1822)影响期间核事故后果评价系统的应用

梁伟鸿　马伟民　吴俊源
香港天文台

摘要

2018年9月16日，超强台风山竹(1822)吹袭广东沿岸，为该区带来猛烈飓风、严重风暴潮及大雨。本文讨论利用香港天文台的核事故后果评价系统，模拟在山竹吹袭时一个假设的核事故情况。分析结果显示，受台风影响的天气状况下，放射性物质在高风速时会被输送得较快，而大雨亦会显著地令较多放射性物质沉积到地面，使空气中放射性物质浓度减低。本文会将这些模拟数据与其他典型天气情况时放射性物质的扩散作比较，为核应急准备提供有用的参考资料。

Applications of Nuclear Accident Consequence Assessment System during the episode of Mangkhut (1822)

LEUNG Wai-hung, MA Wai-man and NG Chun-yuen
Hong Kong Observatory

Abstract

On 16 September 2018, Super Typhoon Mangkhut (1822) hit the coast of Guangdong, bringing violent winds, severe storm surges and heavy rain to the region. This paper discusses the use of the Hong Kong Observatory's Nuclear Accident Consequence Assessment System in simulating the consequences of a hypothetical nuclear accident during the hit of Mangkhut. The results showed that under the weather conditions associated with typhoon, radioactive materials would be transported faster at high wind speeds, and heavy rain would significantly enhance the deposition of radioactive materials onto the ground, leading to a decrease of the concentration of radioactive substances in the air. This paper also compares the simulated data for dispersion of radioactive substances during the episode of Mangkhut with those during a typical weather situation, providing useful references for nuclear emergency preparedness.

1. Introduction

As from the experience of the Fukushima nuclear accident, severe natural disasters, associated with tsunami, tropical cyclones, etc., could be a potential threat to the safety of a nuclear power plant. Should the episode be considered to be an exceptional event with very high impact to the surrounding of the nuclear power plant, there would be a need to carry out emergency preparedness and response actions in anticipation of possible development into a nuclear accident. For emergency preparedness, the potential consequence of a nuclear accident during the hit of a super typhoon should be assessed.

This paper will introduce the features of the Hong Kong Observatory's Accident Consequence Assessment System, and will discuss the results of a simulation study on a hypothetical nuclear accident at the Guangdong Nuclear Power Station in Daya Bay during the episode of Mangkhut in September 2018. The simulated results were also compared with those during a typical weather situation to assess the effect of severe weather on the accident consequence.

2. Accident Consequence Assessment System in HKO

The Hong Kong Observatory (HKO) operates a computer system, which is generically named as Accident Consequence Assessment System (ACAS), for assessing the radiological consequences for Hong Kong in the unlikely event of a radioactive plume release from the Guangdong Nuclear Power Station (GNPS) and Lingao Nuclear Power Station (LNPS) at Daya Bay, or other nuclear power plants in Guangdong. In 2011, HKO adopted the **R**eal-time **O**nline **D**ecisi**O**n **S**upport (RODOS) system to replace the old standalone system for accident consequence assessment. RODOS was developed after the Chernobyl accident and supported by the European Commission's Research and Technological Development Framework Programmes (Raskob and Ehrhardt, 2000; Raskob *et al.*, 2011; Ievdin *et al.*, 2012). It aims at providing a decision support system that can provide guidance for off-site emergency management following a nuclear accident. RODOS has been widely used in European countries.

Currently, the Java-based RODOS, named JRODOS, version *July 2014 Update 3* is in operational use at HKO. This version provides three dispersion models for users' selection, namely ATSTEP (Päsler-Sauer, 2007), RIMPUFF

(Thykier-Nielsen *et al.*, 1999) and DIPCOT (Andronopoulos *et al.*, 2009). A study by Päsler-Sauer (2010) indicated that all three dispersion models produce similar and realistic results under simple and moderately complex meteorological situations. ATSTEP is a Gaussian puff model that releases time-integrated elongated puffs, which are transported along two trajectories attached to both ends of each puff. In RIMPUFF, the puffs are released and tracked with short time steps and it better resembles a continuous release. It takes advection speed into consideration for the puff release rate and the puffs will be split when they are diffused beyond the grid box. Being more advanced, RIMPUFF is more suitable for inhomogeneous flow and changing meteorological conditions. DIPCOT is a particle model which calculates the dispersion using a Lagrangian random-walk approach and turbulent diffusion is modelled as Markov Process. DIPCOT has the capability to produce more realistic results under complex terrain.

In terms of computation speed, ATSTEP is the most efficient one and a study was conducted for its applicability in the Hong Kong situation (Leung *et al.*, 2018). It is currently the default operational dispersion model for use in HKO for nuclear emergency. As DIPCOT is rather computationally demanding, for timeliness consideration, we are considering taking RIMPUFF for operational use in the future. In this study, in view of the changing meteorological conditions associated with Mangkhut, the RIMPUFF model has been used.

3. Methodology and Data of the Hypothetical Case Study

In order to assess the possible consequences in case of a nuclear accident at Daya Bay during the hit of Mangkhut, we make use of the JRODOS RIMPUFF model to simulate a hypothetical airborne radiological release from the GNPS.

Mangkhut came closest to the GNPS around 1 p.m. on 16 September (Figure 1). In the study, it was assumed that radiological release started at 1 p.m. on 16 September. Simulated results for activity concentration and ground deposition of specific radionuclides, effective dose and equivalent dose in thyroid at different distances from the nuclear power plant were calculated. The study also compares the simulated results during the episode of Mangkhut with those during a typical weather situation. The source term and meteorological data are described in details below.

3.1 Source Term Data

Simulations were carried out using JRODOS based on a nominal source term, S3, adopted as a technical basis in France for emergency planning (Charpin *et al.*, 2008). S3 is a conservative source term, and can be considered as a reasonable envelope covering the upper end of the worst foreseeable scenarios, or maximum conceivable release, for nuclear power plants with French designed PWR. It assumes the occurrence of severe accidents with core meltdown and failure of containment, which may be classified at Level 7 of the International Nuclear and Radiological Event Scale (INES) rating. For the iodine group, the release is nearly 1% of the core inventory. Release amounts of the major radionuclide groups of the S3 source term for a 900 MWe PWR (Charpin *et al.*, 2008) are given in Table 1. As a conservative approximation, those values are assumed to be the release amounts of the radionuclides Xe-133, I-131, Cs-137 and Te-132 for this study. A release duration of 12 hours is assumed for the study so that the released plume would be under the effect of high winds and heavy rain associated with Mangkhut.

3.2 Meteorological Data

JRODOS can accept meteorological data through manual input or from numerical weather prediction (NWP) data files.

During routine operation, NWP data from HKO's Meso-scale Non-hydrostatic Model (Meso-NHM) (Wong, 2010) are ingested into JRODOS twice daily based on the 00 UTC and 12 UTC runs. The horizontal grid resolution of the Meso-NHM data is 10 km x 10 km, with a forecast period of up to 72 hours covering southeastern China (18-28ºN, 108-128ºE). For the Mangkhut case study, the simulation was driven by the Meso-NHM data based on the model run at 12 UTC on 15 September 2018. The Meso-NHM forecast wind fields from 06 UTC to 15 UTC on 16 September 2018 are shown in Figure 2.

Simulation with a typical weather situation was also conducted for comparison purpose. A wind speed of 5 m/s, with atmospheric stability class D and no rainfall, was assumed for the typical weather situation. This generally represents an average of the wind speed and atmospheric stability in normal situations. In order to have the change in wind direction on par with the Mangkhut case, the wind direction in the typical situation was assumed to vary between 100^o and 140^o during the prognostic period. The parameters of the typical weather situation are shown in Table 2.

4. Results and Discussion

When Mangkhut hit the coast of Guangdong on 16 September, it brought violent winds and heavy rain to the area. Figure 3 shows the 10-minute mean wind speed and direction recorded at various stations in Hong Kong at 2 p.m. on 16 September 2018, and Figure 4 shows the radar imagery captured at the same time. Storm to hurricane force winds were affecting Hong Kong and heavy rain was affecting the Pearl River Delta at that time. Figure 5(a) is a simulated plume coverage map at 2 p.m. on 16 September, one hour after the release. It can be seen that the radioactive materials have been transported to a distance of about 120 km from the nuclear power plant, which is around three times the distance travelled during the typical weather situation (Figure 5(b)).

Heavy rain would significantly enhance the deposition of radioactive materials onto the ground. Table 3 compares the simulated ground deposition of Cs-137 and I-131 at different distances from the nuclear power plant during the Mangkhut episode and the typical weather situation. During the Mangkhut episode, the simulated ground depositions of Cs-137 and I-131 could be up to about 91 times and 18 times respectively of that under the typical weather situation. It is also noted that the difference near the release source is more significant than those at distances farther away. In JRODOS RIMPUFF, the wet deposition is modelled by multiplying a scavenging coefficient (AI^B, where I is the rain intensity, A and B are constants depending on the characteristics of the radionuclide) with the activity concentration in air (Thykier-Nielsen *et al.*, 1999). Therefore, the efficiency of the wet deposition depends on the rain intensity, the activity concentration in air, and the characteristics of the radionuclide. This essentially explains the observed variations of the deposition pattern in the study.

Under the high winds and atmospheric instability associated with Mangkhut, as well as significant deposition of radioactive materials onto the ground brought by heavy rain, there would be a decrease in the activity concentration of radioactive materials in the air. Table 4 compares the simulated activity concentration of I-131 in the air at different distances from the nuclear power plant during the Mangkhut episode and the typical weather situation. During the Mangkhut episode, the simulated activity concentration of I-131 in the air would be reduced to about 36%-58% of that during the typical weather situation.

This study also evaluates the projected doses at different distances and how far from the nuclear power plant the IAEA generic criteria (IAEA, 2011) would be reached for protective actions to be taken to reduce the risk of stochastic health effects (namely, sheltering/evacuation: effective dose of 100 mSv in the first 7 days; and iodine thyroid blocking: equivalent dose in thyroid of 50 mSv in the first 7 days).

The simulated effective dose and equivalent dose in thyroid at different distances from the nuclear power plant during the Mangkhut episode and under the typical weather situation are shown in Table 5 and Figure 6. During the Mangkhut episode, as a result of the decrease in activity concentration of I-131, there would be less inhalable I-131 in the air. The equivalent dose in thyroid, with major contribution from inhalation of I-131, would be reduced significantly to about 11%-38% of that during the typical weather situation (Table 5). For the typical weather situation, some areas at distances up to around 30 km from the nuclear power plant may meet the IAEA generic criteria for thyroid blocking (Table 5 and Figure 6(b)). During the Mangkhut episode, only some areas at distances up to 10-20 km from the nuclear power plant would meet the IAEA generic criteria for thyroid blocking (Table 5 and Figure 6(a)).

The effective dose is calculated from the sum of the doses from inhalation, cloud shine and ground shine. During the Mangkhut episode, the combined effect of the reduction in inhalable radiation and decrease in cloud shine due to less radioactive materials in the air would cause a decrease in the effective dose. On the other hand, the increase in ground deposition would make a positive contribution to the effective dose. From Table 5, for distances of 10-20 km from the nuclear power plant, there is an increase of about 20% in the effective dose as compared with that during the typical weather situation. The overall increase is due to the positive contribution from the prominent increase in ground deposition close to the nuclear power plant. For distances of 20-90 km from the nuclear power plant, the effective doses are about 18%-93% of that during the typical weather situation (Table 5). This overall decrease in effective dose results from the decrease in positive contribution from ground deposition at farther distances from the nuclear power plant, together with the decrease in cloud shine and inhalable radiation. In both the Mangkhut case and the typical weather situation, the effective doses exceeding the 100 mSv IAEA generic criteria threshold do not go beyond a few kilometres from the nuclear power plant.

5. Concluding Remarks

The consequences of a hypothetical nuclear accident during the hit of Mangkhut have been simulated in this study. Comparison with the simulated results during a typical weather situation showed that heavy rain would significantly enhance the deposition of radioactive materials onto the ground, especially at close proximity of the nuclear power plant. The high wind speed, atmospheric instability and significant deposition would lead to a decrease of the activity concentration of radioactive substances in the air.

In assessing the environmental consequence of accidental releases from nuclear power plants, estimating the ground deposition usually plays an important role, in particular in identifying hot spots and assessing longer term consequence. In this study, it was revealed that the efficiency of wet deposition depends on the rain intensity and the effect of rain is one of the most important mechanisms for high concentration ground deposition. Such phenomenon had also been observed during the Fukushima nuclear accident (Korsakissok *et al.*, 2013).

On the dose assessment perspective, simulation results showed that for areas close to the nuclear power plant, the effective dose during the Mangkhut episode could be slightly larger than that during the typical weather situation, due to the significant contribution from the ground deposition. The effective dose decreases with increasing distance and for distances farther than 30 km from the nuclear power plant, it was in general less than 70% of that during the typical weather situation. For the equivalent dose in thyroid, the decrease is more remarkable for all distances as there is less inhalable radioactive iodine in the air.

The analysis results in this paper may serve as a handy reference in assessing the effects on the accident consequence due to severe weather associated with tropical cyclones. In future studies, a database of different release scenarios under different weather situations may be developed to facilitate quick reference during nuclear emergency.

References

Andronopoulos, S., E. Davakis and J.G. Bartzis, 2009: RODOS-DIPCOT Model Description and Evaluation, RODOS(RA2)-TN(09)-01, https://resy5.iket.kit.edu/RODOS/Documents/Public/HandbookV6f/Volume3/RA2TN0901_DIPCOT.pdf.

Charpin, F., E. Raimond and B. Chaumont, 2008: Technical Basis for Off-site Emergency Panning in France. Int. J. Risk Assessment and Management, Vol. 8, Nos. 1/2.

IAEA, 2011: IAEA Safety Standards Series No. GSG-2, Criteria for Use in Preparedness and Response for a Nuclear or Radiological Emergency, General Safety Guide, International Atomic Energy Agency, 2011.

Ievdin I., O.V. Khalchenkov, W. Raskob, D.M. Trybushny, M.J. Zheleznyak, I.V. Kovalets, 2012: Application of decision support system JRODOS for assessments of atmospheric dispersion and deposition from Fukushima Daiichi nuclear power plant accident, International Journal of Energy for a Clean Environment, 01/2012; 13(1-4):179-190.

Korsakissok I., A. Mathieu, D. Didier, 2013: Atmospheric dispersion and ground deposition induced by the Fukushima Nuclear Power Plant accident: A local-scale simulation and sensitivity study, Atmospheric Environment, Volume 70, May 2013, Pages 267-279.

Leung W.H., W.M. Ma, and Philip K.Y. Chan, 2018: Nuclear accident consequence assessment in Hong Kong using JRODOS, Journal of Environmental Radioactivity, Volume 183, March 2018, Pages 27-36.

Päsler-Sauer, J., 2007: Description of the Atmospheric Dispersion Model ATSTEP, RODOS(WG2)-TN(97)-01, https://resy5.iket.kit.edu/RODOS/Documents/Public/Handbook/Volume3/4_2_5_ATSTEP.pdf.

Päsler-Sauer, J., 2010: Comparison and validation exercise of the three atmospheric dispersion models in RODOS, Radioprotection, Vol. 45, No. 5, 2011, S89-S96.

Raskob, W. and J. Ehrhardt, 2000: The RODOS System: Decision Support For Nuclear Off-Site Emergency Management in Europe, Proceedings of the 10th International Congress of the International Radiation Protection Association, 14-19 May 2000.

Raskob, W., D. Trybushnyi, I. Ievdin and M. Zheleznyak, 2011: JRODOS: Platform for improved long term countermeasures modelling and management, Radioprotection, Vol. 46, No. 6, 2011, S731-S736.

Thykier-Nielsen, S., S. Deme and T. Mikkelsen, 1999: Description of the Atmospheric Dispersion Module RIMPUFF, RODOS(WG2)-TN(98)-02, https://resy5.iket.kit.edu/RODOS/Documents/Public/HandbookV5/Volume3/4_2_6_RIMPUFF.pdf.

Wong, W.K., 2010: Development of Operational Rapid Update Non-hydrostatic NWP and Data Assimilation Systems in the Hong Kong Observatory. Paper presented at the 3th International Workshop on Prevention and Mitigation of Meteorological Disasters in Southeast Asia, 1-4 March 2010, Beppu, Japan, http://www.hko.gov.hk/publica/reprint/r882.pdf.

Nuclide groups	Noble gases	Iodine	Caesium	Tellurium
Total activity released (Bq)	5 x 10^{18}	8 x 10^{16}	2.5 x 10^{15}	1.5 x 10^{16}

Table 1 The French S3 source term for a 900 MWe PWR (Source: Charpin, *et al.*, 2008)

Wind speed (at 10 m height)	Wind direction	Stability Class	Rainfall
5 m/s	100^o to 140^o (during the prognostic period)	D	Nil

Table 2 Parameters of the typical weather situation in the study

Distance from GNPS (km)	Maximum Cs-137 Ground Contamination			Maximum I-131 Ground Contamination		
	Mangkhut episode (A) (Bq/m^2)	**Typical weather situation (B) (Bq/m^2)**	**Ratio (A/B)**	**Mangkhut episode (A) (Bq/m^2)**	**Typical weather situation (B) (Bq/m^2)**	**Ratio (A/B)**
10 - 20	8.79E+06	9.69E+04	91	6.21E+07	3.53E+06	18
20 - 30	3.19E+06	4.46E+04	72	1.99E+07	1.43E+06	14
30 - 40	1.58E+06	3.10E+04	51	9.46E+06	9.80E+05	9.7
40 - 50	9.22E+05	2.33E+04	40	5.46E+06	6.93E+05	7.9
50 - 60	6.16E+05	2.06E+04	30	3.56E+06	5.52E+05	6.4
60 - 70	3.64E+05	1.82E+04	20	2.09E+06	4.69E+05	4.5
70 - 80	2.18E+05	1.73E+04	13	1.28E+06	4.39E+05	2.9
80 - 90	1.48E+05	1.52E+04	9.7	9.26E+05	3.90E+05	2.4

Table 3 Simulated ground deposition of Cs-137 and I-131 at different distances from the nuclear power plant during the Mangkhut episode and the typical weather situation

Distance from GNPS (km)	Maximum activity concentration of I-131		
	Mangkhut episode (A) (Bq/m^3)	Typical weather situation (B) (Bq/m^3)	Ratio (A/B)
10 - 20	8.80E+04	1.52E+05	58%
20 - 30	3.47E+04	7.34E+04	47%
30 - 40	2.33E+04	5.05E+04	46%
40 - 50	1.69E+04	3.78E+04	45%
50 - 60	1.34E+04	3.44E+04	39%
60 - 70	1.20E+04	2.91E+04	41%
70 - 80	9.68E+03	2.69E+04	36%
80 - 90	8.95E+03	2.44E+04	37%

Table 4 Simulated activity concentration of I-131 in the air at different distances from the nuclear power plant during the Mangkhut episode and the typical weather situation

Distance from GNPS (km)	Maximum effective dose			Maximum equivalent dose in thyroid		
	Mangkhut episode (A) (mSv)	Typical weather situation (B) (mSv)	Ratio (A/B)	Mangkhut episode (A) (mSv)	Typical weather situation (B) (mSv)	Ratio (A/B)
10 - 20	10.0	8.34	120%	55.8	148	38%
20 - 30	3.57	3.84	93%	19.9	68.1	29%
30 - 40	1.82	2.67	68%	10.9	47.3	23%
40 - 50	1.11	1.98	56%	7.09	35.2	20%
50 - 60	0.77	1.75	44%	5.24	31.2	17%
60 - 70	0.48	1.55	31%	3.67	27.6	13%
70 - 80	0.32	1.48	21%	2.67	26.4	10%
80 - 90	0.23	1.29	18%	2.50	23.1	11%

Table 5 Simulated effective dose and equivalent dose in thyroid during the Mangkhut episode and the typical weather situation

Figure 1 Track of Mangkhut approaching Hong Kong

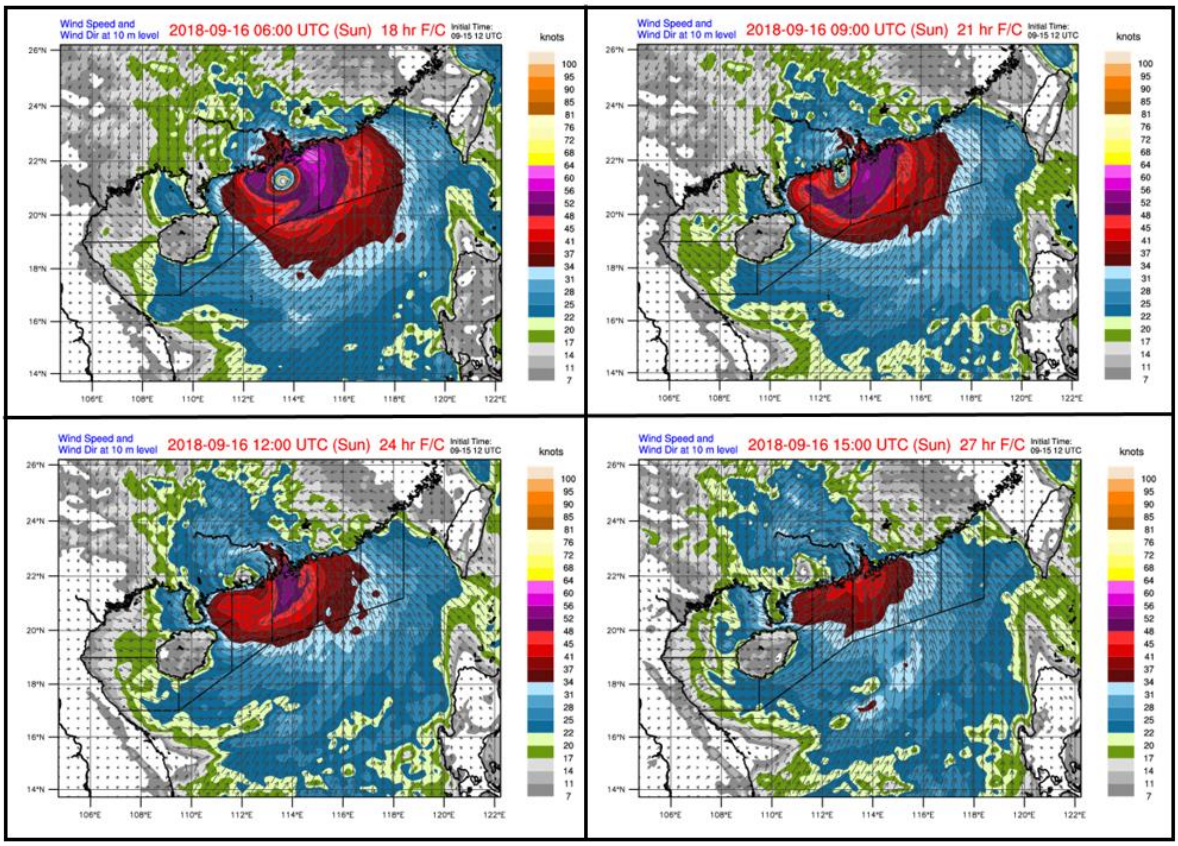

Figure 2 Meso-NHM forecast wind fields from 06 UTC to 15 UTC on 16 September 2018, based on model run at 12 UTC on 15 September 2018

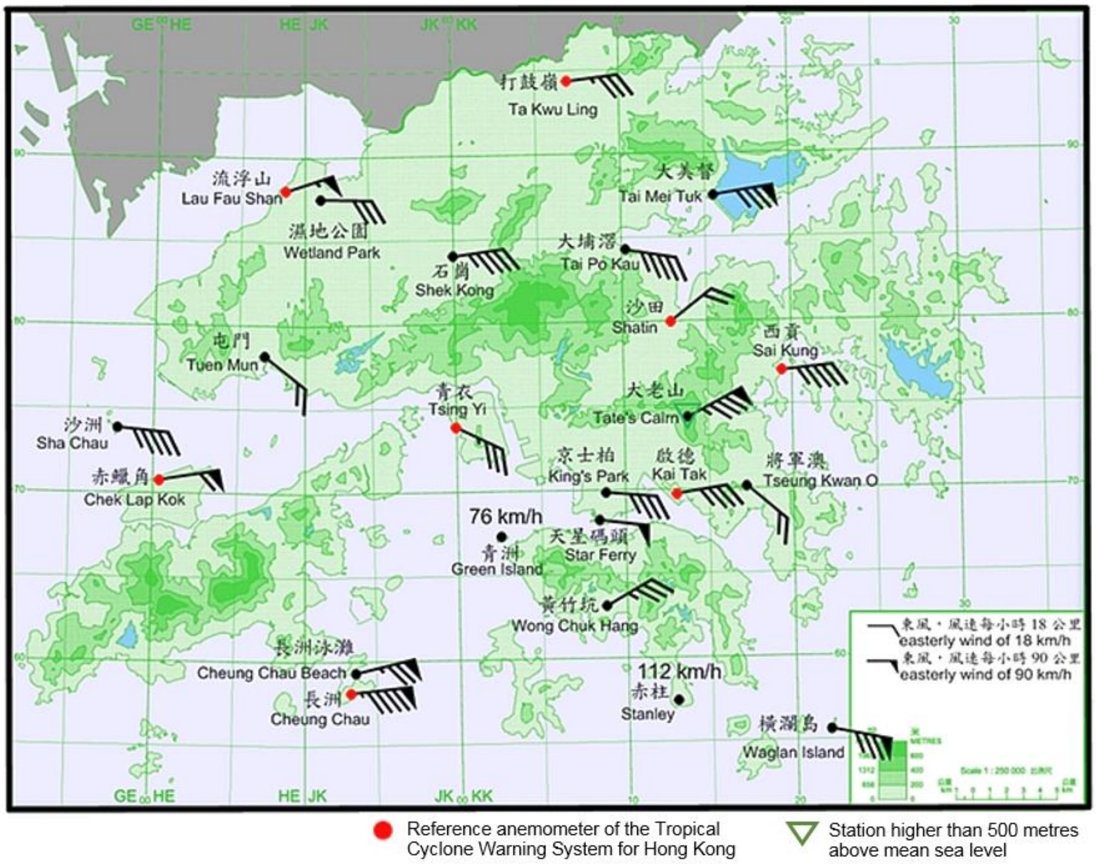

Figure 3 The 10-minute mean wind direction and speed recorded at various stations in Hong Kong at 2 p.m. on 16 September 2018. (Note: Only wind speeds were available at Green Island and Stanley at that time.)

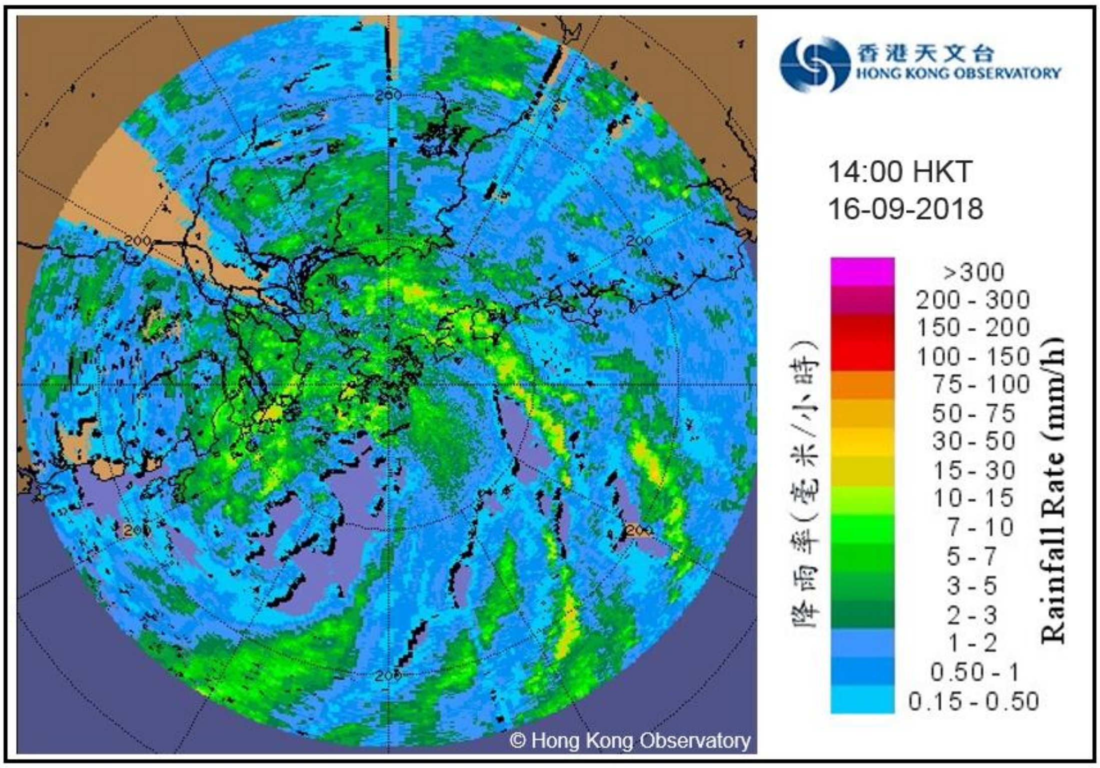

Figure 4 The radar imagery at 2 p.m. on 16 September 2018

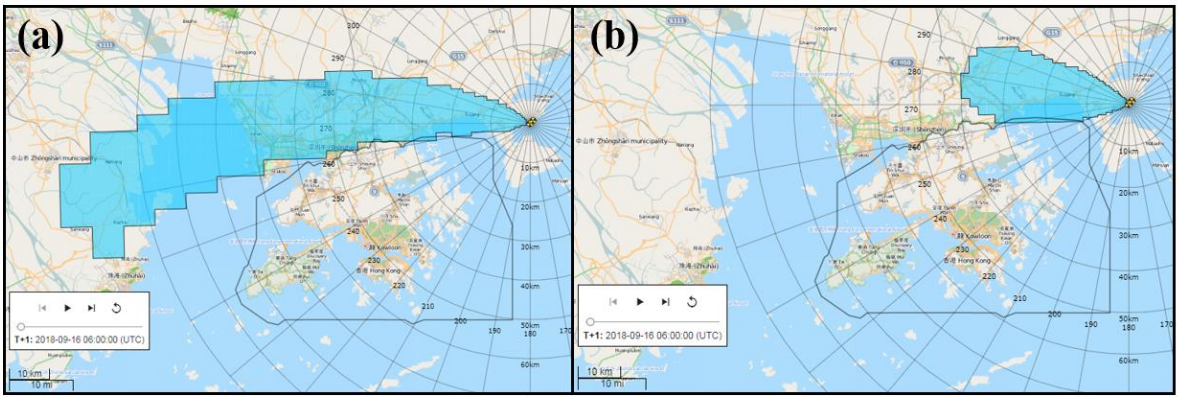

Figure 5 (a) Simulated plume coverage map one hour after release during the Mangkhut episode. The plume was transported to a distance of about 120 km from the nuclear power plant under high winds.
(b) Simulated plume coverage map one hour after release during the typical weather situation. In JRODOS RIMPUFF, winds at upper levels are modelled by extrapolating the winds at 10 m height by an exponential wind speed profile (Thykier-Nielsen *et al.*, 1999). Thus at higher altitudes the plume was advected faster than the wind speed at 10 m height and travelled up to 40 km in this case.

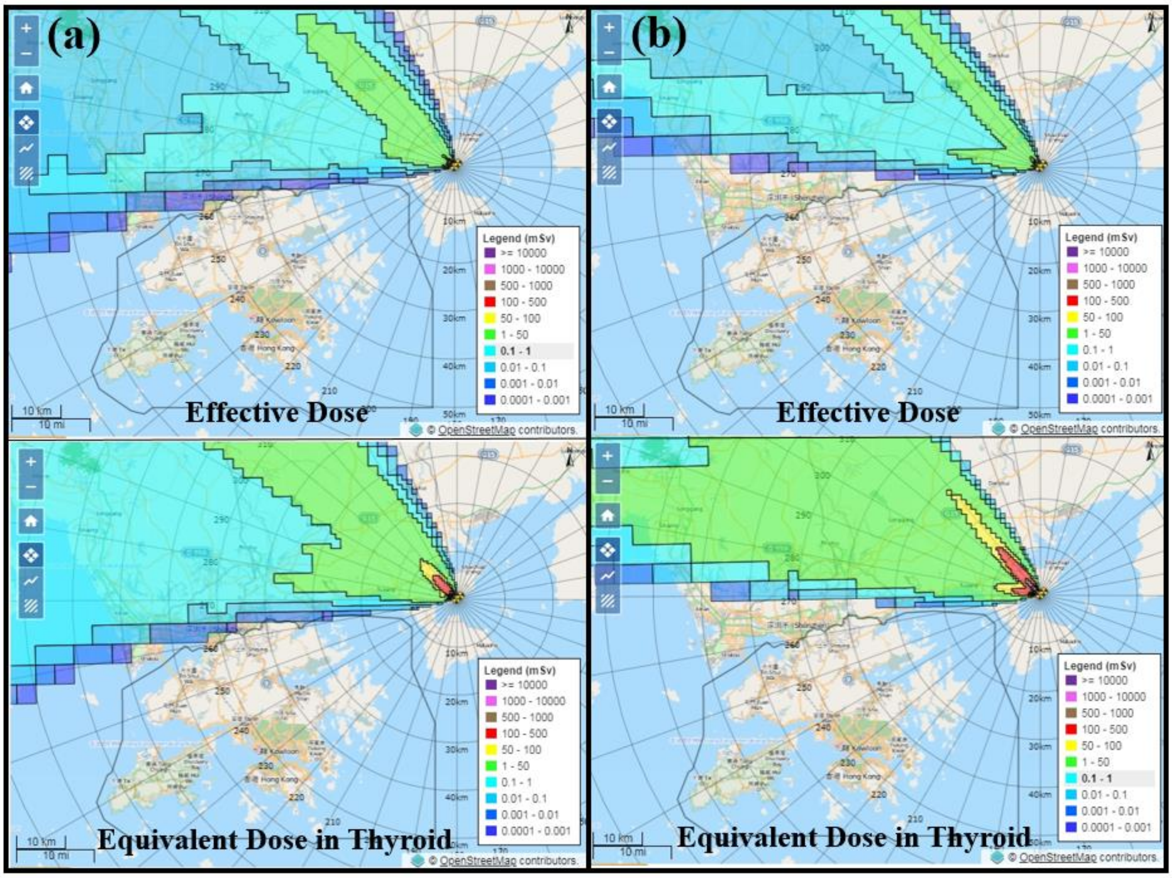

Figure 6 (a) Simulated maps of effective dose and equivalent dose in thyroid during the Mangkhut episode
(b) Simulated maps of effective dose and equivalent dose in thyroid during the typical weather situation